Assimilation of Doppler radar radial winds with HIRLAM 3D-Var

Kirsti Salonen
Finnish Meteorological Institute
kirsti.salonen@fmi.fi

1 Introduction

Interpretation of radar wind measurements is usually obtained through a geophysical inversion, such as VAD or VVP techniques. An alternative method to interpret and to quantitatively exploit radar wind measurements is data assimilation. This consists of modelling the measurement with the Numerical Weather Prediction (NWP) model variables. In data assimilation, the difference between the model counterpart and the observation is minimized. The solution is constrained by the NWP model background and by all available observational information and thus the problem is nearly always well-posed, unlike the case for geophysical inversion.

In this article the observation modelling for the Doppler radar radial winds is described. Section 2 considers the characteristics of Doppler radar radial wind superobservations. Formulation of the observation operator is provided in Section 3 and some test results are given in Section 4. Section 5 considers briefly the future plans.

2 Superobservations

Doppler radars produce radial wind data with high temporal and spatial resolution. The horizontal resolution of the data is around one kilometer whereas the typical resolution of a mesoscale NWP model is of the order of ten kilometers. Doppler radar wind observations thus represent partly phenomena which are not resolved by the NWP model. Calculating spatial averages from the raw data, called superobservations (SO), decreases this representativeness error. Figure 1 displays the radial wind raw data and the corresponding SO with a scale of approximately 10 km. The processing software for SO generation has been developed as an extension to the Radar Analysis and Visualization Environment RAVE (Michelson, 1999).

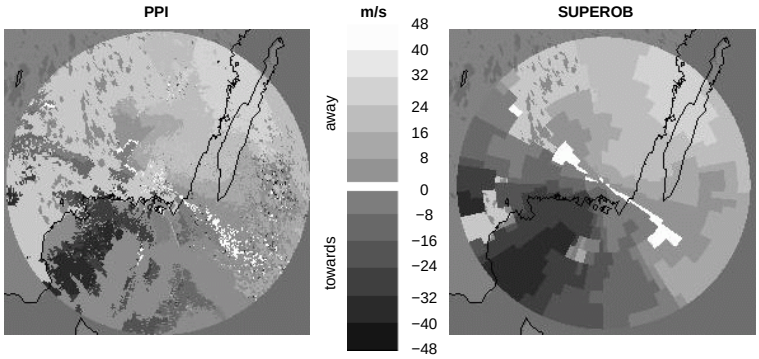

Figure 1: An example of the Doppler radar radial wind raw data (left) and super-observations generated through horizontal averaging (right).

3 Observation operator for Doppler radar radial winds

Three dimensional variational data assimilation (3D-Var) is based on the minimization of the cost function

$$\begin{aligned} J &= J_b + J_o = \frac{1}{2}(\mathbf{x}-\mathbf{x^b})^T\mathbf{B}^{-1}(\mathbf{x}-\mathbf{x^b}) \\ &+ \frac{1}{2}(\mathbf{y}-H\mathbf{x})^T\mathbf{R}^{-1}(\mathbf{y}-H\mathbf{x}), \end{aligned} \tag{1}$$

where J_b measures the distance of the model state vector $\mathbf{x}$ to the background model state vector $\mathbf{x^b}$ and J_o to the observation vector $\mathbf{y}$ respectively (Gustafsson et al. 2001). Observation operator H produces the model counterpart of the observed quantity.

The formulation of the observation operator (Salonen et. al, 2003) for the Doppler radar radial winds involves

1. Horizontal and vertical interpolation of the NWP model wind components u and v to the observation location.

2. Projection of the interpolated NWP model horizontal wind towards the radar, and finally on the slanted direction of the radar beam.

The shape of the radar beam main lobe is approximately Gaussian (Probert-Jones 1962). The broadening of the radar beam can thus be modelled by using Gaussian averaging kernel for the vertical interpolation. Fig. 2 displays the beam broadening and examples of the vertical averaging kernel at ranges of 50 km and 150 km. The Gaussian averaging kernel is non-zero from the Earth's surface up to the top of the atmosphere. Of course, only the wind information which the radar is able to measure should be included into the model counterpart. The obscuring effect of the radar horizon is taken into account by assuming a radar horizon of 0° elevation angle, below which the model information is not used. This lower limit of the averaging kernel is denoted by the lower limit of the shaded region

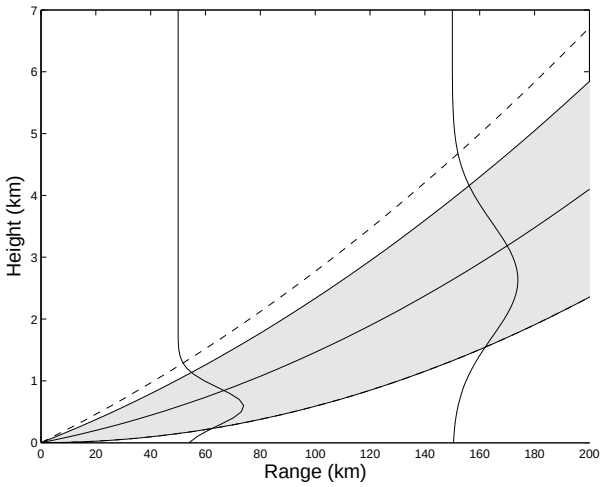

Figure 2: An illustration of the radar beam broadening with 1° beamwidth (shaded area), upper limit for the Gaussian averaging kernel (dashed line) and shapes of the weight function with measurement ranges of 50 km and 150 km. The radar beam elevation angle is 0.5°.

in Fig. 2. An empirical upper integration limit is set to 1.5 times the beamwidth (Jarmo Koistinen, personal communication). This is based on the fact that the radar reflectivity usually decreases rapidly above that height. The upper limit for the averaging kernel is denoted by a dashed line in Fig. 2.

Radar beam bending is taken into account by the Snell's law. The local refraction index is calculated from the NWP model temperature and humidity profiles for model levels assuming horizontal homogeneity between the measurement and the radar location. The total bending of radar beam path across the model levels is accumulated in the observation operator until the radar beam reaches the observation location. The last calculated elevation angle is used in the projection of the horizontal wind on the slanted direction of the radar beam. This modifies also the observation height from the value obtained by applying the $\frac{4}{3}r$-law.

4 Fit of the observations with the model counterpart

A 14 day assimilation experiment has been performed to study the fit of the SO winds with the model counterparts. The observations are from the SMHI radar network with an unambiguous velocity interval of ± 48 m/s. The model counterpart is calculated from the model background state $\mathbf{x^b}$, which is a 6 hour forecast of the FMI operational HIRLAM NWP system. In the SO generation free parameters associated to each observation are stored.

A scatter diagram of SO winds and model counterparts (not shown) reveals that there are outliers in the data. In Fig. 3a is shown the rms difference between the model counterpart and the SO winds as a function of number of polar bins

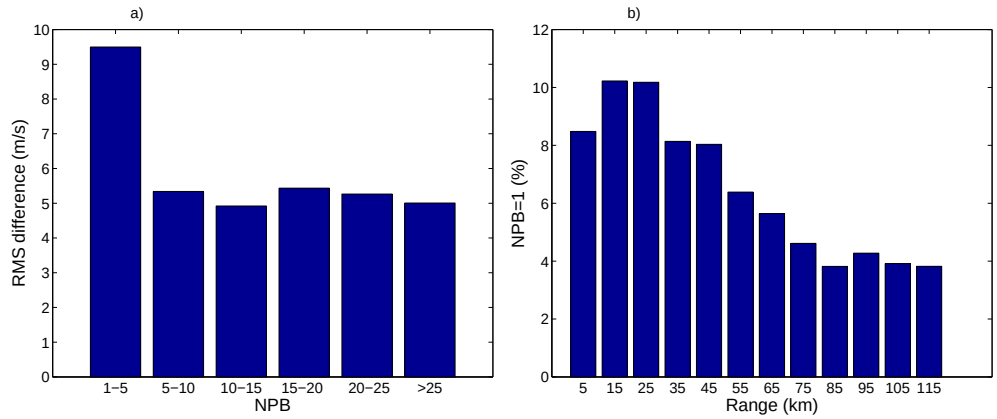

Figure 3: a) Rms difference between the model counterpart and SO winds as a function of NPB. b) Percentage of SO winds generated from one polar bin at different measurement ranges.

(NPB) used in the SO generation. The rms difference is almost twice as large in the class where NPB has a value from 1 to 5 than in other classes. A small value for NPB indicates that the SO originates from few, maybe isolated, data bins and a large value indicates that SO represents more homogeneous coverage of hydrometeors. In Fig. 3b is shown the percentage of SO winds where NPB has the value 1 at different measurement ranges. Up to the range of 45 km the percentage of SO winds generated from only one polar bin is 8-10%. With longer measurement ranges the percentage decreases and from measurement range 75 km it is approximately 4%. The SO winds which strongly deviate from their model counterpart originate thus mainly from the short measurement ranges. The deviating SO winds are most probably observations from nonmeteorological targets such as birds, ships and remaining ground clutter. The outlying data points can be effectively removed by setting quality criteria for NPB, measurement range and the variance of the raw radial wind values forming a SO (VRW). The choise made in this paper is to accept SO data from ranges less than 100 km, with NPB more than 5 and with VRW less than 10 m^2/s^2. The criterion for VRW is chosen to limit the internal variability of the SO to the typical magnitude of the SO itself.

Figures 4 a and b show the fit of TEMP *u*-wind component (Fig. 4a) and SO radial winds (Fig. 4b) to the model counterpart. Generally speaking the TEMP and SO quality with respect to the model background is very similar. TEMP observations vary between approximately $\pm$50 m/s and the SO winds vary between $\pm$20 m/s. This is because TEMP soundings observe higher wind values from higher altitudes than the radar does.

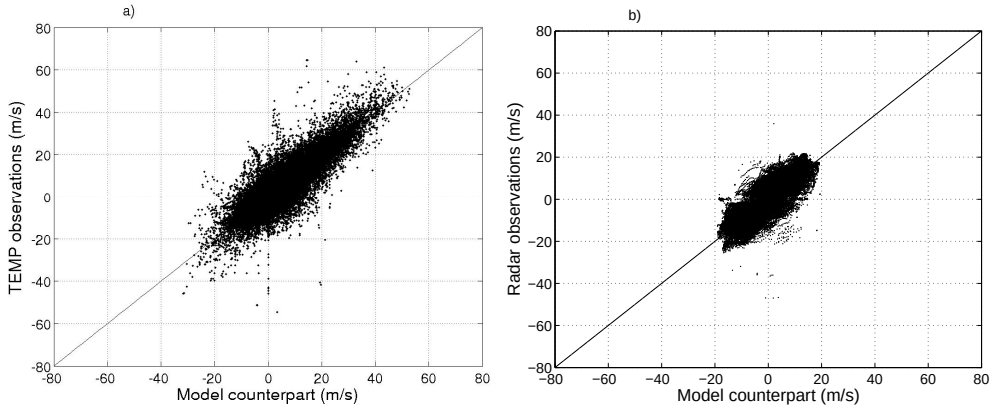

Figure 4: a) Scatter diagram of TEMP observations of wind component *u* as a function of model counterpart. With solid line is shown the ideal fit. b) Same as a) but for SO winds.

5 Future plans

A 10 day parallel assimilation experiment indicates that use of Doppler radar wind information has a positive effect on forecasts especially in the low and middle troposphere (Lindskog et. al, 2003). More extended parallel runs will be performed in the near future to confirm the results. Impact studies of using radar wind data on forecasting severe weather events are also been planned with high priority.

References

Gustafsson, N., Berre, L., Hörnquist, S., Huang, X.-Y., Lindskog, M., Navascués, B., Mogensen, K.S., and Thorsteinsson, S., 2001: Three-dimensional variational data assimilation for a limited area model. Part I: General formulation and the background error constraint. *Tellus*, **53A**, No. 4, 425-446.

Lindskog, M., Salonen, K., Järvinen, H. and Michelson, D. B., 2003: Doppler radar wind data assimilation with HIRLAM 3D-Var. *Monthly Weather Review*, (in press).

Michelson, D. B., 1999: RAVE User's Guide. *Available from SMHI, SE-601 76, Norrköping, Sweden. 51 pp.*.

Probert-Jones, J. R., 1962: The radar equation in meteorology. *Quart. J. Roy. Meteor. Soc.*, **88**, 485-495.

Salonen, K., Järvinen, H. and Lindskog, M., 2003: Model for Doppler radar radial winds. *31st Conference on Radar Meteorology Volume I*, s. 142-145.